Available online at www.sciencedirect.com
ScienceDirect
Procedia Materials Science 6 (2014) 43 – 60
Procedia Materials Science
www.elsevier.com/locate/procedia

3rd International Conference on Materials Processing and Characterization (ICMPC 2014)

EPFM Analysis Of Subsurface Crack Beneath A Wheel Flat Using Dynamic Condition

Nagvendra kumar kanoje[a]*, Satish C. Sharma[a], S.P.Harsha[a]

* Mechanical & Industrial Engineering Department, Indian Institute Of Technology,Roorkee-247667,Uttarakhand,India

Abstract: During running due to frequent braking and suddenly jamming of brakes the Railway wheel skids over rails. This frequent skidding removes large amount of metal from the surface known as Wheel-flat defect. In this paper the wheel-flat and a subsurface crack in the beneath is studied using FEA. If the wheel-flat is not detected early the subsurface crack can originate in the beneath due to inclusion, may leads to fatal accidents. In this study wheel material is taken Elastic-plastic and J-Integral factor has been obtained. The wheel–rail vehicle is modelled as a mass–spring–damper system

Selection and peer review under responsibility of the Gokaraju Rangaraju Institute of Engineering and Technology (GRIET)

Keywords: Wheel-Rail contact, Rolling contact fatigue, Wheel-Flat, FEM, Defects, J-Integral

Nomenclature

ε_Y'	Total strain rate
ε_Y^{e1}	Elastic strain rates
ε_Y^{p1}	Plastic yield rates
α^{dev}	Deviatoric part of Backstress tensor
S	Deviatoric stress tensor
σ_Y'	Backstress tensor values
C_1, γ_1	Kinematic hardening parameter
M_b	Car Body Mass
M_w	Wheel Mass
T	Torque at Axle
K_b	Vertical stiffness
C_b	Vertical damping
K_{pad}	Rail pad stiffness
C_{pad}	Rail pad damping
$K_{sleeper}$	Sleeper stiffness
$C_{sleeper}$	Sleeper damping
$K_{ballast}$	Ballast Stiffness
$C_{ballast}$	Ballast Damping

Selection and peer review under responsibility of the Gokaraju Rangaraju Institute of Engineering and Technology (GRIET)
doi:10.1016/j.mspro.2014.07.007

ρ	Density
E	Young's modulus
ν	Poisson ratio

Corresponding author*: nagvendrakanoje@gmail.com*

1. Introduction

During the braking process in railway transport jamming of brake pads or seizer of wheel causes skidding of wheel continuous for some distance, thus damaging tread which wear excessively at the point of contact with rail and becomes flat to certain length and depth. It is found its length may range typically from 20mm to 100 mm.The rise in temperature caused by abrasion, followed by a fast cooling, may lead to the formation of brittle martensite beneath the flat defect. This is in the origin of further flaws like cracks and spalls with loss of relatively large pieces of tread material. During the manufacturing of wheel either by casting or forging these inclusion get induced in to the matrix of the wheel. During the process the thermal and cooling operation like quenching wheel expands and constrict. Due to this there some residual stresses exists around the inclusion which may further during life cycle due to debonding create crack and failure of wheel.

Kumagai et al. (1991) investigated the occurrence of Wheel-flat due to brake shoe and give range of surface roughness. Dukkipatti and Dong (1999) studied characteristics of the impact loads due to wheel-flats and shells are investigated based on the validated FE model of railway track. The track is represented by a Timoshenko beam on discrete pad-tie-ballast supports. When the wheel rolls represented by a Timoshenko beam on discrete pad-tie-ballast supports. When the wheel rolls over a flat, it develops high impact forces that may cause further damages to the wheel and rails studied by Vyas and Gupta (2006). Furthermore, above a critical speed, a loss of rail-wheel contact occurs, which produces increased noise and vibrations was found by Wu and Thompson (2002). Wheel-flats are amongst the most common local surface defects of railway wheels. The repetitive high impact forces involved cause a rapid deterioration of both, rolling and fixed railway structures.

Sackfield, et al. (2007) obtained the pressure distribution for all orientations of the flat under quasi-static conditions. Dong and Dukkipati (1994) studied the steady-state response of a vehicle-track system for a wheel with flat as defect carrying a constant load and travelling at a constant speed over a track with no irregularities is studied using the FEM model. The impact loads due to wheel flats are also studied with this model. Baeza et al. (2006) analyse the influence of the elastic wheel-rail contact model, to determine the dynamic response caused by a geometric irregularity (in rail or wheel) by means of Hertzian and non-Hertzian contact models with an example of wheel flat. Steenbergen (2008) given the classification of wheelflats according to the different stages of their growth is given, along with the characteristic features of the dynamic wheel–rail interaction for each category and obtained the relationship between the impact magnitude and the train speed.

A practical approach to simulate the practical condition many vehicle model has been published of which some are referred below. Rajib et al. (2007) given an analytical model of the coupled vehicle-track system by integrating a pitch plane model of the vehicle with a two-dimensional model of the flexible track comprising 3-layers together with a nonlinear rolling contact model and studied the impact forces due to wheel flats and its effect on motions and forces transmitted to vehicle and track components. Rajib et al. (2008) employed a non-linear Hertzian contact theory to accomplish the dynamic interactions between the lumped mass vehicle and the continuous rail and studied the effect of one wheel flat. Xin et al. (2007) a three-dimensional dynamic vehicle-track finite element (FE) model has been created to investigate the dynamic stress state of the rail surface and the effects of the tangential contact force. Hyun et al.(2011) present a newly developed three-dimensional nonlinear coefficient of friction (CoF) model for the dry rail condition with the help of wheel–rail modelled as a mass–spring–damper system to simulate the basic wheel–rail dynamics.

In this study a literature review is also done on subsurface crack and its propagation. Lin et al. (2005) suggested a method to detect the crack initiation point of charpy pre-cracked specimen under dynamic loading and

obtained the dynamic fracture toughness. Glodez et al. (2005) presented a computational model for simulation of surface and subsurface initiated fatigue crack growth due to contact loading and applied the virtual crack extension method using finite element method to simulate crack growth. Colombo et al. (2008) used a precise meshing technique based on an elliptical coordinate transformation that starts from a circular crack and obtained the stress intensity factors K_I, K_{II},and K_{III}. Taraf et al. (2010) did the parametric studies are carried out with a two-dimensional elastic–plastic finite element model of a part of a wheel containing defects. Yongming and Mahadevan (2007) give a new mixed-mode threshold stress intensity factor is developed using a critical plane-based multiaxial fatigue theory and the Kitagawa diagram. An equivalent stress intensity factor defined on the critical plane is proposed to predict the fatigue crack growth rate under mixed-mode loading. Chwan et al. (1993) studied the transient problem of a half-space containing a subsurface inclined semi-infinite crack subjected to normal impact on the boundary of the half-space. Guduru et al. (1998), studied the dynamic crack initiation in ductile steels (Ni-Cr steel and 304 stainless steel) at different loading rates and to establish appropriate dynamic failure criteria. Arne Melander (1997) studied the crack propagation considering five inclusion configurations in terms of crack-tip displacements and energy release rates. MI Guo-fa et al. (2011) employed Goodier equation to analyze the stress state around inclusion and cavity in the operation of wheel-rail contact stress and conclude with the size and depth of the inclusion. Johan et al.(2011) found the probability of occurrence of subsurface initiated rolling contact fatigue cracks in the vicinity of the material defects considering mean defect size. Elena et al. (2011) developed a new criterion for real-time assessment of subsurface RCF from measured wheel–rail contact forces and also compared it to previous simplification of the Dang Van equivalent stress criteria. Yongming et al.(2007) calculated stress intensity factors using a three-dimensional elasto-plastic finite element model in which a sub-modeling technique is used to achieve both computational efficiency and accuracy. Wallentin et al. (2005), studied the cracks originate from wheel flats as induced by wheel/rail sliding and found Stress intensity factors for modes I, II and III assuming linear elastic conditions. They do analysis on both 2D and 3D model and found that the stress intensity factor in Mode II and III is greater than Mode I.

As with the increase in axle load stresses may reach to plastic limit. Many work has been done to study the stresses in elastic-plastic condition and also their influence on crack propogation. Thomas et. al.(1983) conducted elasto-plastic finite element analyses of freight car wheel, subjected to cyclic thermal load and mechanical load and computed the fatigue life with the help of stresses and strain. Bower A. F. et al. (1991) described a simple non-linear kinematic hardening law for predicting the plastic flow that occurs when the shakedown limit is exceeded to study the response of rail steel to sliding contact loading. Yanyao Jiang et al. (1996) proposed a new plasticity model studied the residual stresses and progressive shear strain ratchetting for the line rolling contact problems utilizing a recently developed semi-analytical approach. They found that the ratcheting rate of rolling surface movement rapidly decreases with increasing number of rolling passages (cycles) and ratcheting continues for many cycles. Yu C.-C. et al. (1996) applied a three-dimensional elastic-plastic rolling-sliding contact problem on a quarter space to approximate wheel-rail contact. It is a highly efficient technique for the determination of the steady state solution, such as residual stress, residual strain, and the cyclic strain range, under proportional or non-proportional cyclic loading and may be used to predict fatigue life. Yanyao Jiang et al.(2002) conducted a Finite element Three-dimensional elastic-plastic rolling contact stress analysis simulations to study the influences of the tangential surface forces in the two shear directions on residual stresses and residual strains and given a comparisons with the two-dimensional rolling contact model.Wen Z. F. et. al.(2006) used an advanced cyclic plasticity model and commercial finite element code via a material subroutine found that for any given creepage including zero value, when the number of rolling passes increases, the surface depth of the wavy-deformed surface increases but the ratcheting rate decays.Zefeng Wen et. al. (2011) used A finite element model and advanced cyclic plasticity theory and studied wheel-rail contact stresses and found that a wavy surface profile evolves due to plastic deformation on rail surface with rolling history and tends to stabilize due to the decaying ratcheting rate. Lei Wu et al. (2011) studied thermal-elastic–plastic deformation and residual stress with the help of a finite element method (FEM) for a wheel sliding on a rail. Shashidhar et al. (2010) use a elastic-plastic finite element analyses to presents an effect of specimen thickness on crack-tip plastic zone shape and size and found that maximum plastic zone size occurs beneath the free surface.

Several methods have been put forward for detection of wheel-flat in past. Vittorio et al. (2006) given a diagnostic tool using wavelet transform which are able to detect and to quantify the wheel-flat. Jose et al. (2010) Fritsch (2011) has given an inspection system which analysis the rail-wheel contact by frequency and phase shifts. The difference between the emitted and the received frequency will change if any defect on wheel tread is detected. Brizuela et al. (2011) presents an innovative ultrasound technique designed to detect and quantify flats formed in the rolling wheels.

In this paper a subsurface crack below Wheel-flat induced due to presence of the three types of inclusion has been studied. The major driving factor which is responsible for crack nucleation and growth is J-integral for elastic-plastic material is obtained. A FEM model of crack has been studied under the tread of wheel under the influence of practical condition generated due to dynamics of vehicle system and wheel-rail interaction.

2. **Finite Element Modelling**

For doing simulation first understand well the formulation of wheel-rail interaction given by Xin (2007) and the contact model . In the present problem wheel is moving on the rail with some angular velocity, vehicle load is transmitted from body to the rail by axle, wheel, wheel-rail interaction. The wheel assumed to be fixed with axle by hub and there is no slipping between them, it comes under axle load through the hub. A 3D model of wheel and rail for wheel with wheel-flat defect are simulated in the FEM software ABAQUS to practical conditions subjected to boundary conditions such as speed, load and interaction and vehicle dynamic model given by Hyun (2011) to obtain contact and its effect and significance on the subsurface crack from Yongming (2007) present below the wheel-flat.

In the present problem, wheel with a flat defect is moving on the rail with angular velocity of the wheel, vehicle load is transmitted from body to the rail by axle, wheel, wheel-rail interaction. The wheel assumed to be fixed with axle by hub and there is no slipping between them, it comes under axle load through the hub. A 3D model of wheel and rail is studied. First the simulation is done for contact interaction for fresh wheel-flat defect referred from Baeza (2006) using the FEM software ABAQUS to practical conditions subjected to vehicle dynamic conditions such as speed, coach load and interaction to obtain contact pressure and its effect and significance on the wheel under defect.

2.1 Cyclic plasticity model

The cyclic plasticity model that has been employed in the current study is ABAQUS' combined model with nonlinear isotropic/kinematic hardening given in Innotack (2006) which is based on the work of Lemaitre and Chaboche. In the model the total strain rate is composed from the elastic and plastic strain rates

$$\varepsilon_Y^{'} = \varepsilon_Y^{e1} + \varepsilon_Y^{p1} \tag{1}$$

with the elastic part modeled as linear elastic and the plastic yield surface defined by the function

$$f(\sigma - \alpha) = \sigma^0 \tag{2}$$

where

$$f(\sigma - \alpha) = \sqrt{\frac{3}{2}(S - \alpha^{dev}) : (S - \alpha^{dev})} \tag{3}$$

where α^{dev} is the deviatoric part of the backstress tensor and S the deviatoric stress tensor. The evolution of the backstress tensor is defined as

$$\sigma_Y^{'} = \frac{C_1 \varepsilon_Y^{'p1}}{\sigma^0}(\sigma - \alpha) - \gamma_1 \alpha \varepsilon_Y^{'p1} + \frac{\alpha C_1^{'Y}}{C_1} \tag{4}$$

with C_1 and γ_1 being material parameters.

The following parameters required for the Cyclic plasticity model as follow:

• Yield stress at zero plastic strain- 443.0 MPa

• Kinematic hardening parameter, C_1- 40995.0 MPa

• Kinematic hardening parameter, γ_1- 58.0 or less

The above values are taken estimate 50% of the values obtained by Fedel et. al. (2005) so that plasticity property should be moderate.

2.2 Vehicle Dynamic Model

For studying the contact conditions the formulation of wheel-rail interaction and the contact model has been understood. This paper focuses on the rolling contact between a wheel and a rail with "flat" as a defect, half vehicle-track system has been modelled only in the vertical direction. The schematic diagram of the model is shown in Figure 1. The Z-axis is defined along the longitudinal direction (the rolling direction of the wheel). The carbody and bogie sprung mass are lumped into one rigid body M_b connected to the wheel with suspension springs K_b and dampers C_b; pad, sleepers and ballast are modelled as springs K_{pad}, $K_{sleeper}$, $K_{ballast}$ and dampers C_{pad}, $C_{sleeper}$, $C_{ballast}$ and are reduced to equivalent spring and mass damper name K_{track} and C_{track}. The rail is grounded and the K_{track} and C_{track} are attached at two points below the track at distance equal to the distance between two sleeper i.e 0.6 m.

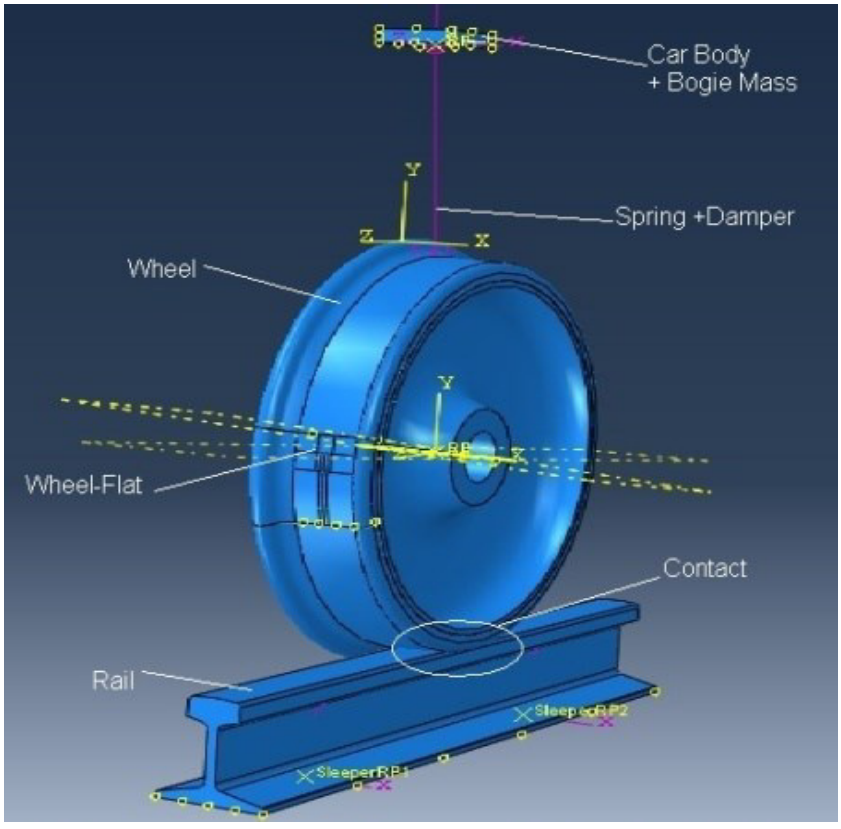

Fig 1. A FEM model for Wheel-rail interaction with the car body mass using mass-spring-damper model.

Table1: Vehicle, rail, track and material parameters .

S.No.	Parameters	Symbols	Values
Load-Coach parameter [16]	Car Body Mass	Mb	4450(kg)=44145 (KN)
	Wheel mass	Mw	210 Kg
	Torque at Axle	T	350 N
Suspension [16]	Vertical stiffness	Kb	550×10^3 (N/m)
	Vertical damping	Cb	35×10^3 (Ns/m)
	concrete Sleeper distance	Dist	0.6(m)
Track (maximum value) [16]	Rail pad stiffness	Kpad	110×10^6 (N/m)
	Rail pad damping	Cpad	98×10^3 (Ns/m)
	Sleeper stiffness	$K_{sleeper}$	100×10^6 (N/m)
	Sleeper damping	$C_{sleeper}$	98×10^3 (Ns/m)
	Ballast stiffness	$K_{ballast}$	200×10^6 (N/m)
	Ballast damping	$C_{ballast}$	245 × 103 (Ns/m)
	Distance Between Sleepers	L	0.6 m
Material Parameters for steel [15]	Density	ρ	7850(kg/m^3)
	Young's modulus	E	2.1×10^{11} (N/m^2) or 210Gpa
	Poisson ratio	v	0.3

The equivalent parameters have been obtained for the present vehicle interaction model:

$$\frac{1}{k_{track}} = \frac{1}{k_{pad}} + \frac{1}{k_{sleeper}} + \frac{1}{k_{ballast}} = 41.51E6\ N/m \tag{5}$$

$$c_{track} = c_{pad} + c_{sleeper} + c_{ballast} = 441E3\ Ns/m \tag{6}$$

2.3 Wheel Defect "Flat" Modeling

The wheel has been divided in to three parts like hub and web, rim and wheel-flat after partition of the standard wheel in ABAQUS. This is shown in figure 3. For simulation we have taken wheels with fresh formed flat defect. The parameters has been given below in Table-2.

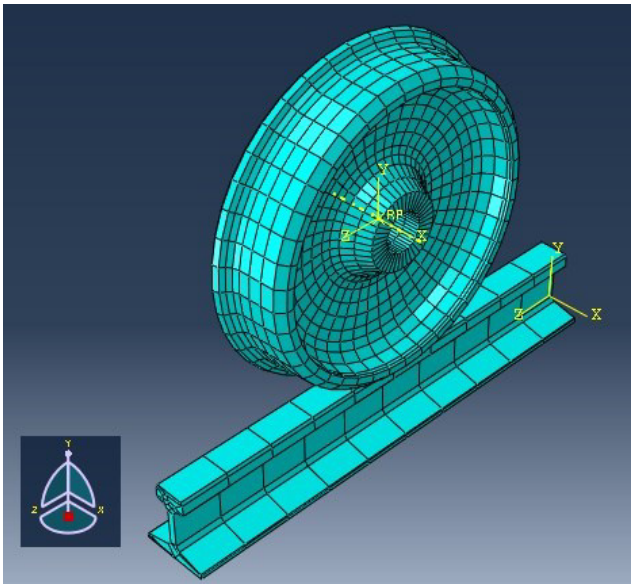

Fig 2. A Normal Wheel meshed in ABAQUS software.

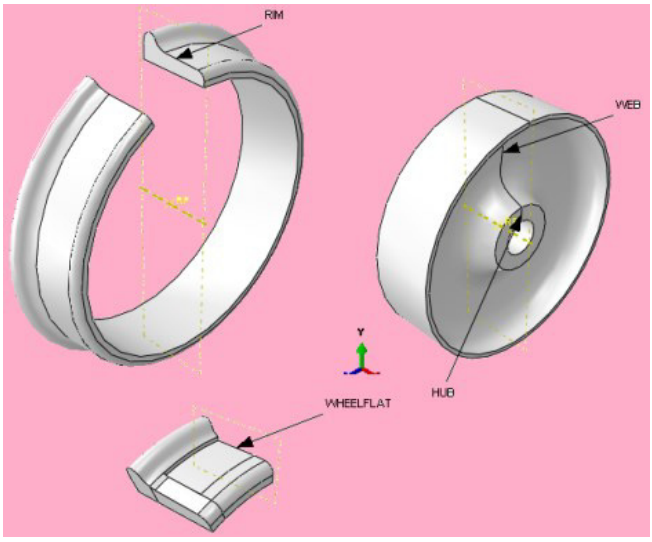

Fig 3. Modeling of Wheel in to three parts- rim, hub and wheel-flat.

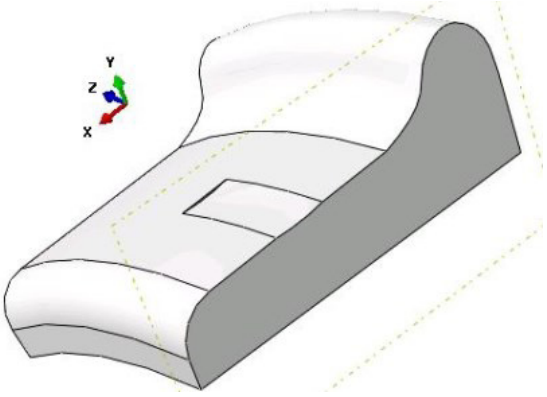

Fig 4: A cut portion of Wheel showing the grove like defect called Wheel-flat.

Table2: Type of Wheel-flat parameters[12].

S. No.	Type	Dimension	Depth(m m)
1	Fresh-Flat (Round)	20X40	0.625

The locomotive wheel with diameter φ =0.62m type Association of American Railroad (AAR) and the rail type International Union of Railway (UIC 60), as shown in Fig. 2 and Fig. 3, are modelled using the constant stress solid element. The material for wheel and rail is elastic-plastic. Very fine mesh is made over rail, wheel and wheel flat defect in order to get sufficient computational accuracy. An dynamic implicit integration method is used to solve the problem in the time domain. The values of some parameters used in the model are listed in Table 1. Coulomb friction law is employed and the coefficient of friction is set to 0.3.

2.4 Crack Modelling

In this paper, the previous used finite element model for subsurface crack propagation analysis is used to find stress intensity factor for subsurface crack below wheel-flat defect. Here crack is of an elliptical shape with dimension taken length of 5 mm shown in Figure. The radius of major arc and radius of minor arc are in ratio 2:1.

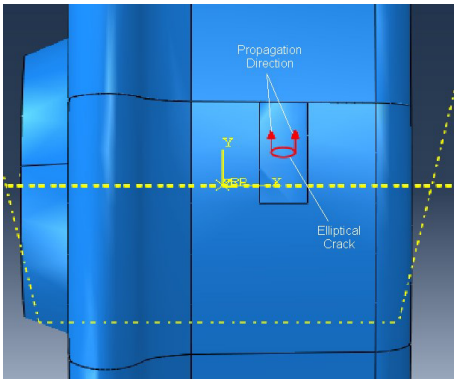

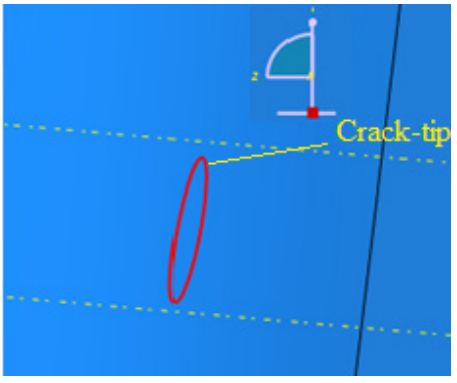

Figure (a) Figure (b)

Fig 5: (a) Subsurface Crack beneath Wheelflat, (b) Elliptical crack in red

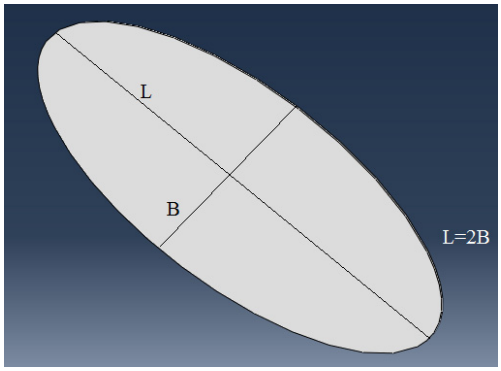

Fig 6. An Elliptical shape subsurface crack.

Table 3: Properties of Inclusion referred from MI Guo-fa (2011)

Type	Density (kg/m^3)	E (GPa)	Poisson's Ratio (v)	Coeff of Thermal Expansion(α)
MnS (Manganese Sulphide)	3990	390	0.25	18X10^{-6}
Al_2O_3 (Aluminium Oxide)	4000	390	0.25	8X10^{-6}
TIN (Titanium Nitride)	5400	320	0.19	9.4X10^{-6}
Matrix (R260 STEEL)	7850	210	0.3	10X10^{-6}

The Subsurface crack are basically originated due to inclusion present in the wheel rim and these crack propagate during the service life of the wheel. In this paper three types of inclusion are considered and their property is given in Table 3. In the FEM model we assign the property of the inclusion to the crack and Stress Intensity Factors are obtained.

2.5 Finite Element Model

First the vehicle dynamic model and wheel-flat geometry are incorporated in a 3D global model considering standard wheel and rail and are simulated for stresses and contact parameters in ABAQUS software for small displacement. Meshing is done on global model with C3D8R solid element. Load of vehicle is transferred to a driver node with the help of spring damper connected at the centre of the wheel to the driver node. The driver node is connected to the wheel by rigid element. The boundary condition of the wheel is specified at driver node which automatically gets transfer to wheel during simulation. The simulation is run with a dynamic implicit method for global model constitute whole vehicle model and wheel-rail interaction and stresses are saved in the output file.

The result from global model is fed in to FEM sub-model in the ABAQUS software using output file. In the sub-model, a refined mesh part of the wheel-flat part is taken and an elliptical subsurface crack is introduced in to it below 6 mm depth from the tread surface taken by Yongming et al (2007). The subsurface crack is modelled as two contact surfaces to prevent the surface penetration of the sub surface crack for given contact property. The crack edge is selected crack front same as crack tip line and a virtual propagation direction is given which is parallel to the crack face. The crack is meshed with C3D20R element with an aspect ratio of 0.5

so to perform in crack singularity. The results of global model are imposed on the Wheel-flat nodes induced with a crack and simulation is run for getting stress intensity factor at crack tip nodes.

3. Results and Discussion

3.1 Finite Element Method Results

3.1.1 Results for global model

The simulation has been run for global model incorporating vehicle dynamic model as in Fig. 1 and wheel-flat geometry in Figure 4 using a standard wheel and rail geometry in ABAQUS software.

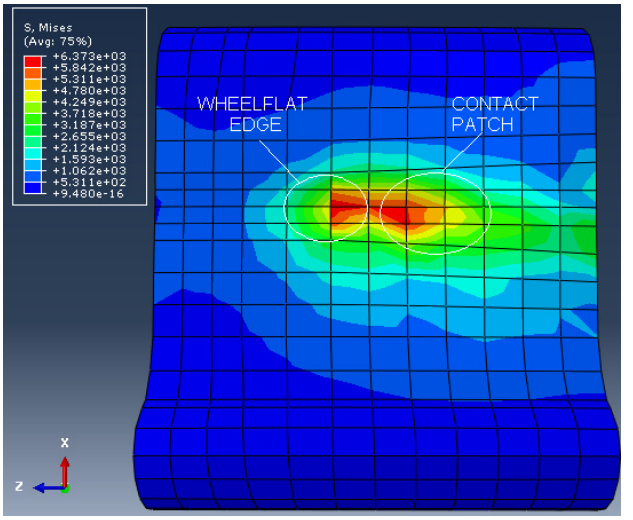

Fig. 7. Contact stresses on Wheel-flat portion.

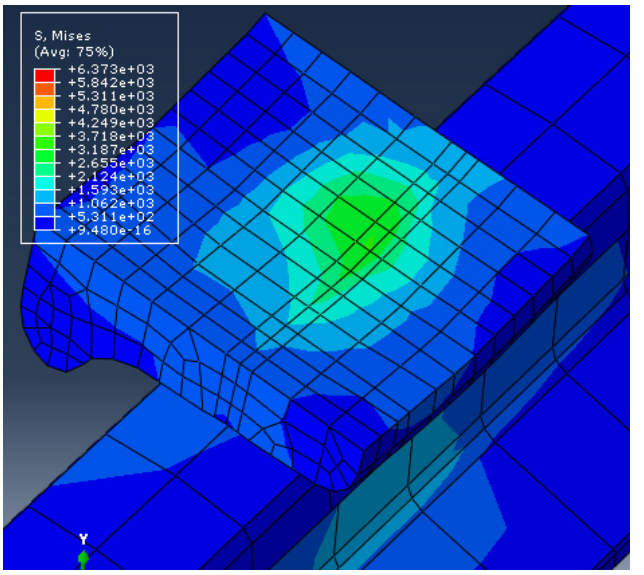

Fig. 8. Von Mises stress over the width of wheel-flat portion.

In the above Figure the contact stresses are shown. The bigger red spot is the contact patch and the smaller red spot the stresses generated at the end of the Wheel-flat in Fig. 7. Fig. 8 showing the stress distribution back of the wheel-flat part. This shows the stresses are high enough around the crack when induced just below the wheel-flat surface.

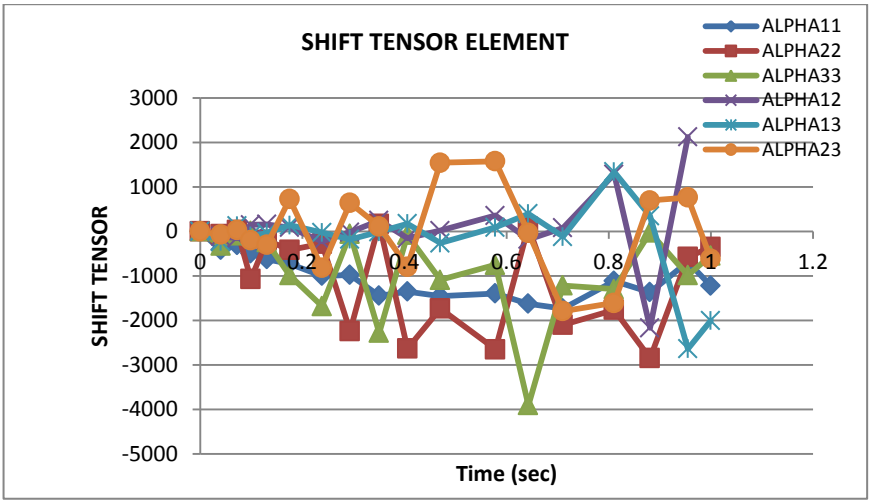

Fig 9. Showing variation of diagonal components of the deviatoric part of the backstress tensor.

For studying the nature of stress and strain we have taken a element near to the crack tip just below the wheel-flat surface where crack will be implant in the submodel. The following properties of the element are Element 186: Linear hexahedron, type C3D8R,Nodal connectivity: 17, 28, 144, 109, 441, 442, 747, 749.

Fig. 9. gives the variation of diagonal components of the deviatoric part of the backstress tensor. The backstress components evolve most during the first cycle as the Bauschinger effect overcomes the initial hardening configuration. Only the deviatoric components of the backstress are obtained using ABAQUS. Since the plasticity model considers only the deviatoric part of the backstress. The variation is obtained for single backstress. This shows that all the normal components are of compressive nature and the shear component are varying in a cyclic nature. This shows shear component are of fatigue nature.

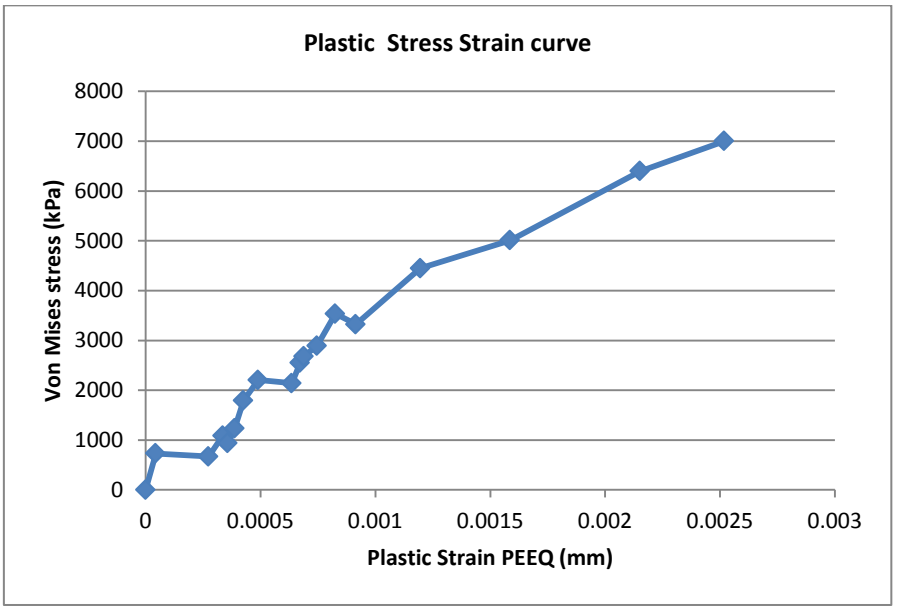

Fig. 10. Variation of Von Mises stress versus Equivalent Plastic strain on a node on Wheel-flat.

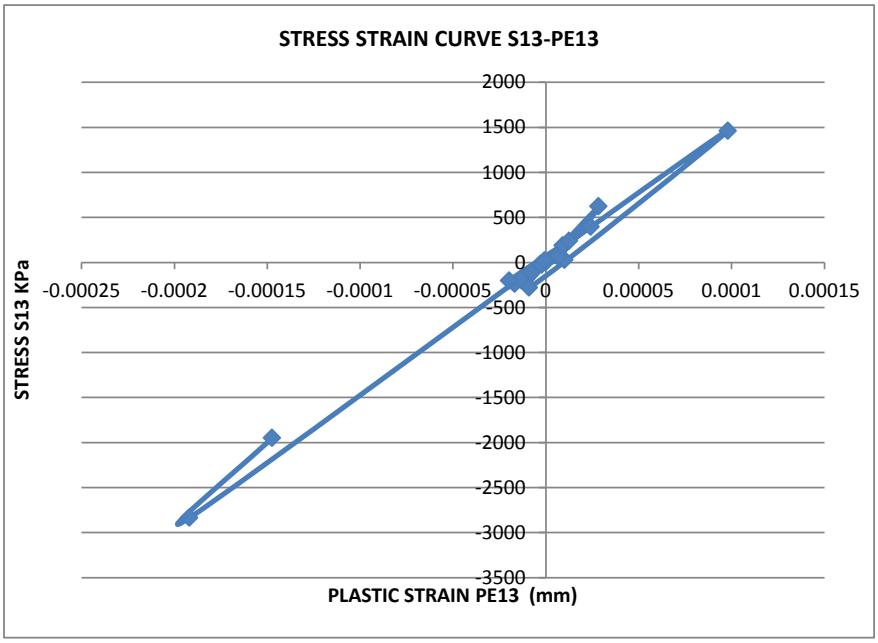

Fig. 11. Variation of stress S13 versus Plastic strain PE13 on a node on Wheel-flat.

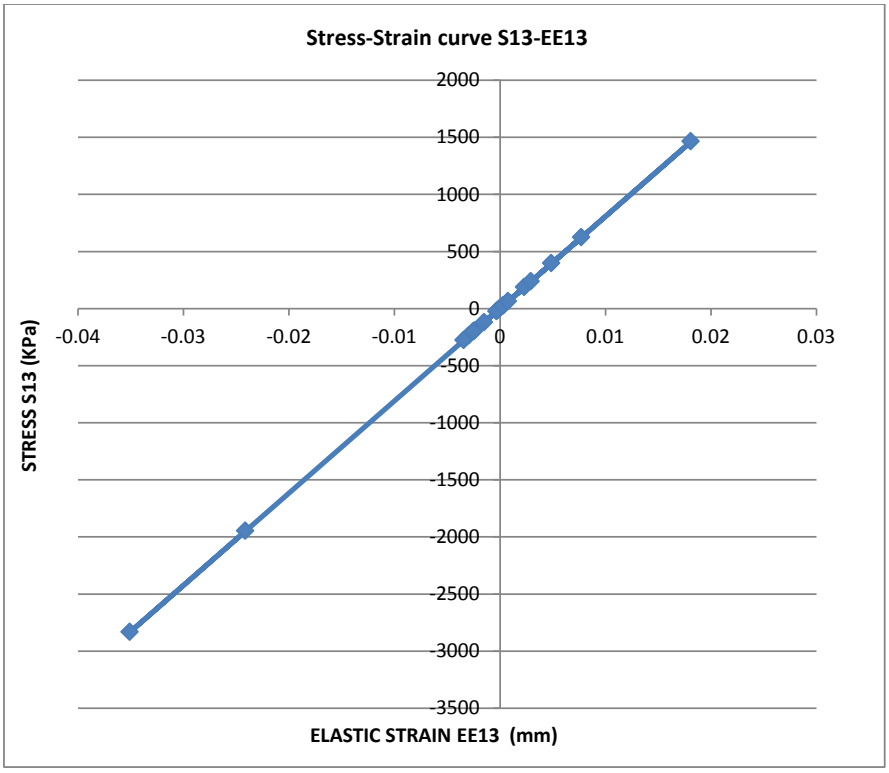

Fig. 12. Variation of stress S13 versus Elastic strain EE13 on a node on wheel-flat.

As the analysis is done for Elastic-Plastic material of the wheel, the backstress tensor all the normal component are of compressive nature but only shear component are of cyclic nature. Figure 11 and 12 shows the variation

of one of the shear component versus respective strain component for single backstress. This shows that the elastic stresses are of linear nature but the plastic stresses are of cyclic nature for one hysteresis cycle.

3.1.2 Results for Sub-model

The results from global model are fed in to sub-model FEM model in the ABAQUS software using output file. For crack propagation the important factor is J-Integral when the material is Elastic-Plastic. In this work the J_1 values are found is also known as first contour Integral. This value of J-Integral tells about the energy release rate when a crack propagates. Different inclusions are considered and J-integral values are found at their node points for different crack orientation from the tangent drawn to the tread surface.

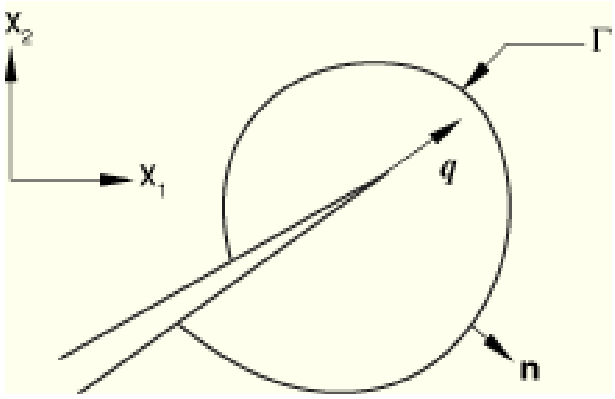

Fig. 13. Contour for evaluation of J integral around a crack tip, where q(propagation direction), n(normal), Γ (Contour)

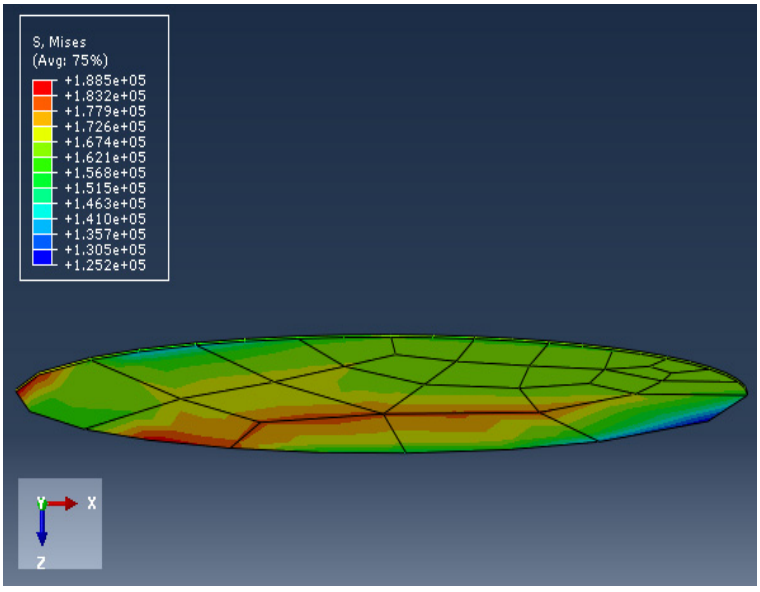

Fig. 14. Stresses at Inclusion (crack) and crack tip.

The Fig. 14 showing the stresses at crack tip. The crack tip of the crack is at very high stress. Due to difference in thermal expansion of the inclusion (as crack) and metal of tread as matrix, inclusion expands and constricts which finally induce a crack in matrix. This crack due to cyclic stresses propagates inside the surface of tread.

3.1.3 The J-Integral for Elastic-Plastic material

It have been obtained for different inclusion and are compared for the value of J-integral. Basically the maximum value of J-integral is considered for the crack propagation.

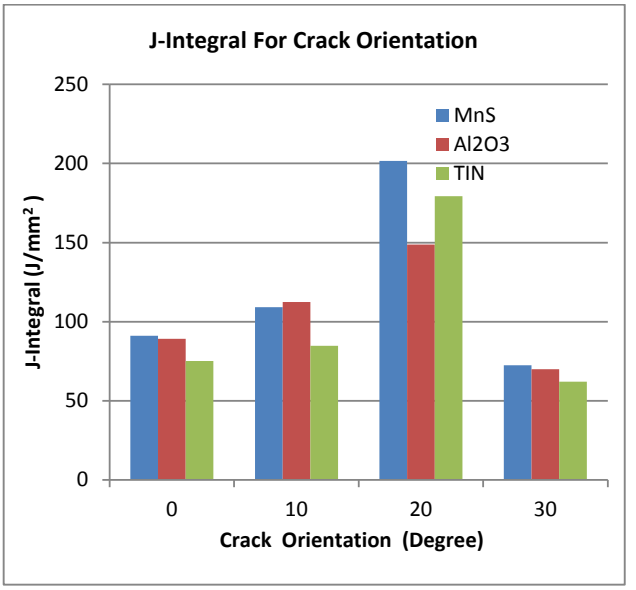

Fig. 15. Crack orientation effect on SIF range (at 3 m/s, 4500kg ,crack size 5mm).

From Fig. 15 we found that as the crack orientation changes there is slight increase in Energy release rate. All the inclusion show steep increase in J-integral when the crack is inclined at 20 deg. Of all these inclusion MnS show highest value of energy release rate at all the crack orientation as compare to other inclusions. Al_2O_3 also show significant increase in Energy release rate. This shows that crack is more likely to grow when the inclusion and the direction of propagation is inclined close to 20 deg to the tangent on the wheel tread surface.

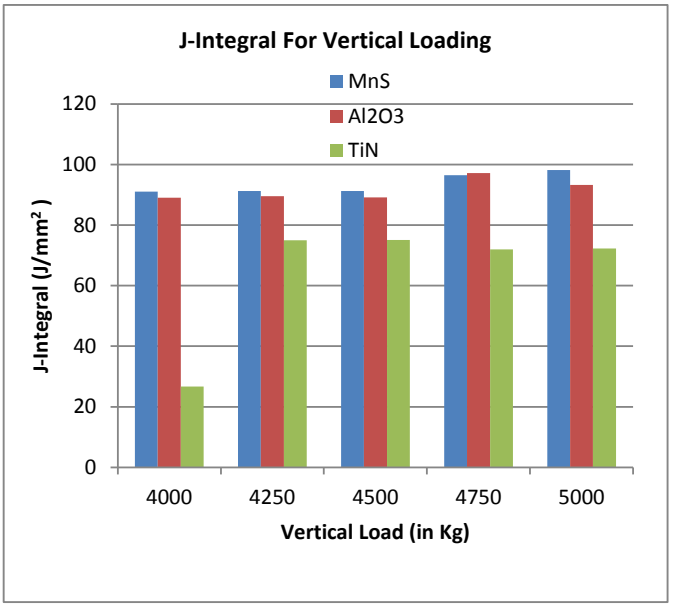

Fig. 16. Vertical Loading effect on SIF range (at 20 m/s, 0 deg orientation, crack size 5mm)

From Figure 16 we found that the Al_2O_3 and MnS both showing significant increase in J-Integral value. At different variations in vertical load MnS shows always increase in Energy release rate. This shows that MnS will likely to help in crack initiation and propagation in an Elastic-Plastic material.

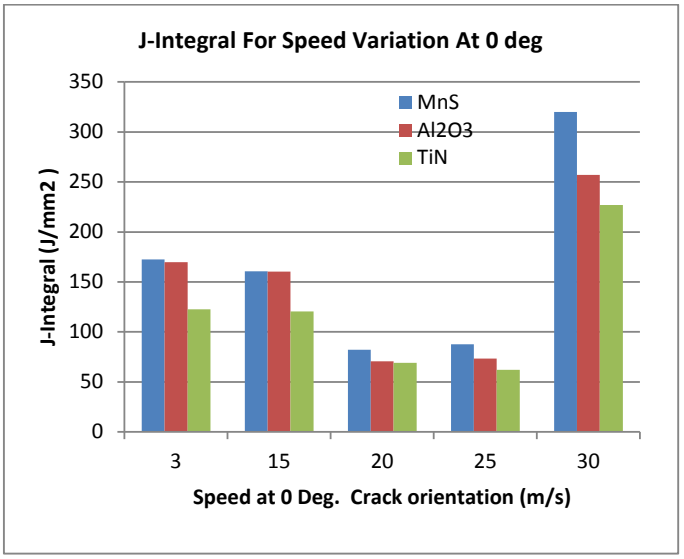

Fig. 17. Speed at 0 Deg Crack orientation effect on SIF range (at angle 0 deg, 4500kg, crack size 5mm)

From Fig. 17 we found that at lower speed that there is almost static condition prevails for the stresses around a crack due to which the crack is more likely to propagate because of more Energy Release rate. At higher speed due to high stresses there is more chances of crack propagation. This graph also shows that that at average speed crack Energy Release rate is less and that's why crack will not propagate more easily. The Al_2O_3 is showing consistent value but MnS is showing tremendous increase in SIF shows that crack will propagate more easily at higher speed.

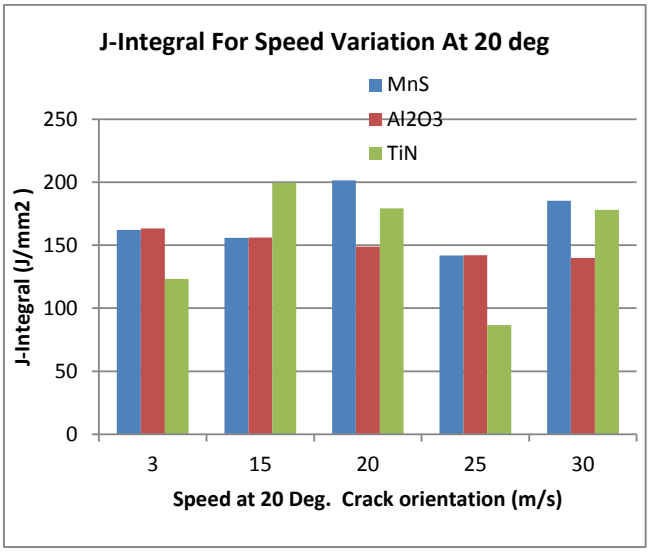

Fig. 18. Speed at 20 Deg Crack orientation effect on SIF range (at angle 20 deg, 4500kg crack size 5mm)

From Fig. 18 shows that the Al_2O_3, MnS and TiN all are showing significant increase in Energy Release rate. This shows that all the inclusion at 20 deg more likely to initiate and propagate a crack in Elastic-Plastic material.

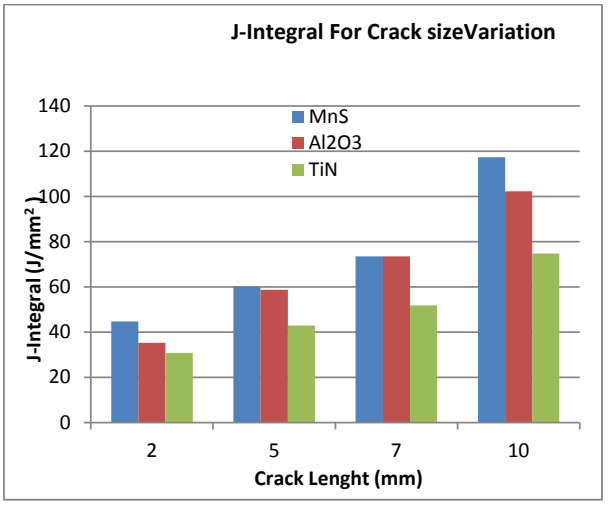

Fig. 19. Crack length effect on SIF range (at 20 m/s and 0 deg at 4500 kg at depth 6mm)

From Fig. 19 give an idea that the MnS is showing consistent increase in Energy Release rate in comparison to Al_2O_3. But both Al_2O_3 and MnS is more likely to initiate a crack because there is very less difference in J-integral value. When the inclusion size increases is of MnS is more likely to initiate a crack in the matrix of the wheel rim and will help in crack propagation.

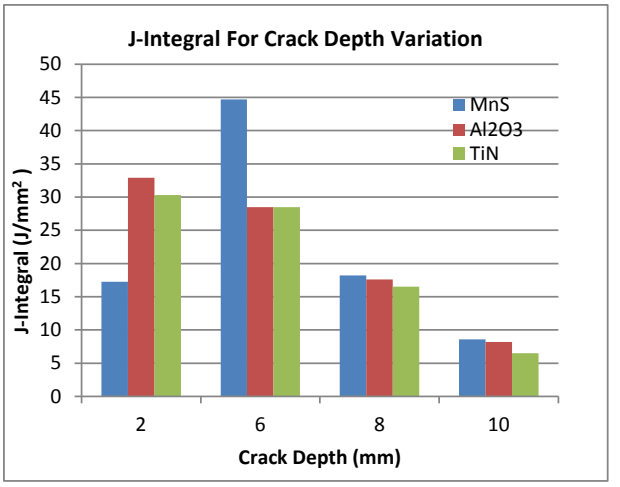

Fig 20: Crack depth effect on SIF range (at 20 m/s, 0 deg at 4500kg, crack size 2mm)

Fig. 20 give an idea that the Al_2O_3 is more sensitive to stress around the wheelflat and can initiate crack at any depth in comparison to MnS because it is showing high J-Integral value. But according to Yongming [23] any crack at the depth of 6 mm shows crack propagation. From these results MnS shows significant high energy release rate when it is at 6 mm depth and is more likely to initiate and propagate a crack in a Elastic- Plastic material.

4. Conclusion

With the use of kinematic hardening model and Elastic-Plastic material of wheel, there was more scope to study stresses around crack. The subsurface crack is prominent and can be originated any time during the life cycle. In this work the comparison of J-Integral value or Energy Release rate for different inclusion gives an idea that the crack originated due to presence of inclusion when their orientation is 20 deg to the tangent to wheel tread just below the wheel-flat surface are more prominent during the life cycle of wheel when especially wheel material

is Elastic-Plastic. The presence of MnS inclusion is more like to show a consistent growth in J-Integral value as compare to Al_2O_3 and it can induce crack more easily in the tread of the wheel during life cycle and also helps the crack propagate the crack easily by inducing stresses. All the inclusion gives high J-Integral value for an inclined crack. The J-Integral value decreases as the crack depth increases.

References

A. F. Bower and K. L. Johnson, 1991, *Plastic flow and shakedown of the rail surface in repeated wheel-rail contact*, Wear, 144, pp. 1-18.

Arne Melander, 1997, *A finite element study of short cracks with different inclusion types under rolling contact fatigue load*, Elsevier, Int. J. Fatigue Vol. 19, No. I, pp. 13-24.

A.Sackfield , D.Dini, D.A.Hills, 2007*Contact of a rotating wheel with a flat*, Inter. J. of Solids and Structures 44, pp.3304–3316.

Brizuela J., Fritsch C., Ibáñez A, 2011, *Railway wheel-flat detection and measurement by ultra sound*, Elsevier, Transportation Research Part C 19, , pp. 975–984.

C.-C. Yu, L.M. Keer, B. Moran, 1996, *Elastic-plastic rolling-sliding contact on a quarter space,* Wear 191,219-225.

Chwan-Huei Tsai, Chien-Ching Ma, 1993, *The stress intensity factor of a subsurface inclined crack subjected to dynamic impact loading*, In,. J. Solid Structure Vol. 30, No. 16, pp. 2163-2175.

Colombo C., Guagliano M., Vergani L., 2008, *A numerical analysis of flat internal cracks under mixed mode loading,* Elsevier, Theoretical and Applied Fracture Mechanics, ,pp. 5066–73.

D. Hibbitt, B. Karlsson, P. Sorensen, 2010, *ABAQUS/Standard User's Manual*, Version 6. 10, ABAQUS, Inc., Pawtucket, RI.

D. J. Thompson, 1993, *Wheel Rail Noise Generation, Part-II, Wheel Vibration*, Journal of Sound and Vibration, 161(3), , pp.401-419.

Elena Kabo, Roger Enblomc, Anders Ekberg, 2011, *A simplified index for evaluating subsurface initiated rolling contact fatigue from field measurements,* ELSEVIER, Wear 271,pp. 120–124.

Fedele R., Filippini M., Maier G., 2005, *Constitutive model calibration for railway wheel steel through tension–torsion tests*, Elsevier, Computers and Structures 83, pp.1005–1020.

Glodez S., Abersek B., Fajdiga G. and Flasker J. 2005, *Computational Analysis of Surface and Subsurface Initiated Fatigue Crack growth due to Contact Loading*,Tech Science Press, SID, vol.1, no.3, pp.215-224.

Guduru P.R., Singh R.P., Ravichandran G. and Rosakis A.J., 1998, *Dynamic crack initiation in ductile steels*, Pergamon, J. Mech. Phys. Solids, Vol. 46, No.10, pp 1997-2016.

Hyun Wook Lee, Corina Sandu & Carvel Holton, 2011, *Dynamic model for the wheel-rail contact friction*, Veh. Sys. Dyn.: International Journal of Vehicle Mech. and Mob,, Volume 50, Issue 2, pp.1–23,iFirst

INNOTRACK report D4.3.5, 2006, *Simulation of material deformation and RCF*, Project no. TIP5-CT-2006-031415O

Jose Brizuela, Alberto Ibanez, Patricia Nevado , Carlos Fritsch, 2010, *Railway Wheel Flat Detector using Doppler Effect*, Elsevier, Physics Procedia, , pp.811–817.

Johnson, K.L., 1985, *Contact Mechanics*, Cambridge University Press, Cambridge, UK,.

Johan Sandström, Jacques de Maréb, 2011, *Probability of subsurface fatigue initiation in rolling contact*, Elsevier, Wear 271,pp.143–147.

Kumagai N., Ishikawa H., Haga K., Kigawa T., Nagase K., 1991, *Factors of wheel flats occurrence and preventive measures*, Wear, 144, pp.277-287.

Lei Wu, Zefeng Wen, Wei Li, Xuesong Jin, 2011, *Thermo-elastic–plastic finite element analysis of wheel/rail sliding contact*, Elsevier, Wear 271,pp. 437–443.

Liming Liu, 2008, *Modeling of Mixed-mode fatigue crack propagation*, PhD Thesis ,Graduate School of Vanderbilt University.

L. Baeza, A. Roda, J. Carballeira and E. Giner, 2006, *Railway Train-Track Dynamics for Wheelflats with Improved Contact Models*, Springer, Nonlinear Dynamics , 45, pp.385–397.

Lin Junshan, Yan Wenbin, Tu Mingjing, 1992, *Crack initiation point determination and dynamic fracture toughness for charpy pre –cracked specimen*, ACTA Metallurgica Sinica (English Edition) Series A, Vol. 5 No. 5, (sep 1992) pp 379-384.

MI Guo-fa , Nan Hong-van, Liu Yan-lei, , Zhang Bin, Zhang Hong, Song Guo-xiang, 2011, *Influence of Inclusion on Crack Initiation in Wheel Rim*, Journal of Iron and Steel Research, Intern., 18(1) , pp. 49-54.

Michaël J.M.M. Steenbergen, 2008, *The role of the contact geometry in wheel–rail impact due to wheel flats: Part II*, Vehicle System Dynamics, 46:8, pp.713-737.

Rao V Dukkipati & Renguang Dong, 1999, *Impact Loads due to Wheel Flats and Shells*, Veh. Sys. Dyn., 31:1, pp.1-22.

R.G. Dong and Rao V Dukkipati , 1994 *A finite element model of railway track and its application to the wheel flat problem*, Proc Instn Mech Engrs Vo1208, IMechE, , pp-61-72.

Rajib Ul Alam Uzzal, Waiz Ahmed and Subhash Rakheja, 2007, *Dynamic analysis of pitch plane Railway vehicle-track interactions due to wheel flat*, Proceedings of the International Conference on Mechanical Engineering 2007 (ICME2007) 29- 31 December, Dhaka, Bangladesh, ICME07-AM-51.

Rajib Ul Alam Uzzal, Waiz Ahmed and Subhash Rakheja, 2008, *Dynamic analysis of railway vehicle-track interactions due to wheel flat with a pitch-plane vehicle model,* Journal of Mechanical Engineering, Vol. ME39, No. 2, (December 2008) ,pp.86-94.

Ramanan L., Krishna Kumar R., Sriraman R., 1999, *Thermo-mechanical Finite element analysis of a rail wheel*, Pergamon, Inter. J. of Mech. Sci. 41, 487-505.

Simha N.K., Fischer F.D., Shan G.X., Chen C.R., Kolednik O., 2008,*J-integral and crack driving force in elastic–plastic materials*, J. of the Mech. and Phy. of Solids 56, pp.2876– 2895

Shashidhar K. Kudari and Krishnaraja G. Kodancha, 2010, *3D finite element analysis on crack-tip plastic zone*, Multicraft, Inter. J. of Engg., Science and Technology, Vol. 2, No. 6, pp. 47-58.

Taraf M., Zahaf E.H., Oussouaddi O., Zeghloul A., 2010, *Numerical analysis for predicting the rolling contact fatigue crack initiation in a railway wheel steel*, Elsevier, Tribology International 43 , pp. 585–593.

Thomas T. J. , Nairs S. And Vijay K. Garg, 1983, *Elasto-Plastic Stress Analysis And Fatigue Life Prediction Of A Freight Car Wheel Under Mechanical And Cyclic Thermal Loads*, Computer & Stuctures, Vol. 17. No. 3., pp. 313-320.

T. Suzuki, M. Ishida, K. Abe, and K. Koro, 2005, *Measurement on dynamic behavior of track near rail joints and prediction of track settlement*, Q.Rep. Railway Technol. Res. Inst. 46, pp.124–129.

Vittorio Belotti, Francesco Crenna, Rinaldo C. Michelini, Giovanni B. Rossi, 2006, *Wheel-flat diagnostic tool via wavelet transform*, Elsevier, Mech. Sys. and Signal Process., 20, , pp.1953–1966.

Vyas, N.S., Gupta, A.K., 2006, *Modeling rail wheel-flat dynamics*, In: Engineering Asset Management. Springer, London, pp.1222–1231.

Wallentin M., Bjarnehed H.L., Lunden R., 2005, *Cracks around railway wheel flats exposed to rolling contact loads and residual stresses*, Elsevier, Wear 258, pp.1319–1329.

Wu, T.X., Thompson, D.J., 2002, A *hybrid model for the noise generation due to railway wheelflats.* Journal of Sound and Vibration, 251(1), pp.115–139.

Xin Zhao, Zili Li, Coenraad Esveld, Rolf Dollevoet, 2007, *The Dynamic Stress State of the Wheel-Rail Contact*, Proceedings of the 2nd IASME/ WSEAS Intern. confer. on continuum Mech. (CM'07), Portoroz, Slovenia, May 15-17, pp. 127-133.

Yongming Liu, Sankaran Mahadevan, 2007, *Threshold stress intensity factor and crack growth rate prediction under mixed-mode loading*, Engineering Fracture Mechanics 74, 332–345.

Yongming Liu, Liming Liu, Sankaran Mahadevan, 2007,*Analysis of subsurface crack propagation under rolling contact loading in rail road wheels using FEM*, Elsevier, Engineering Fracture Mechanics 74, pp.2659–2674

Yanyao Jiang, Huseyin Sehitoglu , 1996, *Rolling contact stress analysis with the application of a new plasticity model*, Wear 191, pp.35-44.

Yanyao Jiang, Biqiang Xu, Huseyin Sehitoglu, 2002,*Three-Dimensional Elastic-Plastic Stress Analysis of Rolling Contact*, Journal of Tribology, ASME OCTOBER, Vol. 124/ 699.

Z. F. Wen and X. S. Jin, 2006, *Elastic-Plastic Finite-Element Analysis of Repeated, Two-Dimensional Wheel-Rail Rolling Contact under Time-Dependent Load*, Proceedings of the Insti. of Mech. Engineers, Part C: J. of Mech. Engg. Sci., 220, pp. 603-613.

Zefeng Wen, Lei Wu, Wei Li, Xuesong Jin, Minhao Zhu, 2011, *Three-dimensional elastic–plastic stress analysis of wheel–rail rolling contact*, Elsevier, Wear 271, pp. 426–436.